metals

MDPI

Article

Disassembly of Li Ion Cells—Characterization and Safety Considerations of a Recycling Scheme

Jean Marshall [1], Dominika Gastol [2], Roberto Sommerville [2], Beth Middleton [1], Vannessa Goodship [1] and Emma Kendrick [2,*]

1 WMG, University of Warwick, International Manufacturing Centre, Coventry CV4 7AL, UK; Jean.Marshall@warwick.ac.uk (J.M.); B.Middleton@warwick.ac.uk (B.M.); V.Goodship@warwick.ac.uk (V.G.)
2 School of Metallurgy and Materials, University of Birmingham, Edgbaston, Birmingham B15 2TT, UK; d.a.gastol@bham.ac.uk (D.G.); R.Sommerville@bham.ac.uk (R.S.)
* Correspondence: e.kendrick@bham.ac.uk; Tel.: +44-121-414-6730

Received: 15 May 2020; Accepted: 5 June 2020; Published: 9 June 2020

Abstract: It is predicted there will be a rapid increase in the number of lithium ion batteries reaching end of life. However, recently only 5% of lithium ion batteries (LIBs) were recycled in the European Union. This paper explores why and how this can be improved by controlled dismantling, characterization and recycling. Currently, the favored disposal route for batteries is shredding of complete systems and then separation of individual fractions. This can be effective for the partial recovery of some materials, producing impure, mixed or contaminated waste streams. For an effective circular economy it would be beneficial to produce greater purity waste streams and be able to re-use (as well as recycle) some components; thus, a dismantling system could have advantages over shredding. This paper presents an alternative complete system disassembly process route for lithium ion batteries and examines the various processes required to enable material or component recovery. A schematic is presented of the entire process for all material components along with a materials recovery assay. Health and safety considerations and options for each stage of the process are also reported. This is with an aim of encouraging future battery dismantling operations.

Keywords: batteries; reuse; recycling; disassembly; safety

1. Introduction

Predicted sales of electric vehicles will create large volumes of end-of-life (EoL) lithium ion batteries (LIBs). Within the European Union, in 2016 it was reported that just 5% of LIBs were being recycled. [1] It is a significant challenge to create an economically viable process for the reclamation of all materials from used batteries and to re-use all of the recovered materials and components. [2,3] The automotive manufacturer remains responsible for the disposal of EoL battery packs, which is complicated by the fact that these are both expensive to ship due to safety issues and may end up in the waste stream in varying states of health.

It is, therefore, imperative to develop a well-understood and safe process for the efficient dismantling of LIBs in such a manner that the valuable materials they contain may be re-used or reclaimed. This is part of the larger circular economy picture for battery recycling and addresses some of the hierarchy of recycling process decisions illustrated previously by Harper et al [4].

In order to develop a safe recycling process, the battery must first be stabilized by being discharged to a known state of charge (SOC) [5] The SOC is defined according to the capacity that can be delivered by the battery/cell with respect to its value in the charged state. The SOC is not defined by the cell voltage, however the cell voltage can be used to infer the SOC. The exact end-of-discharge voltage required to attain SOC = 0% varies with the internal resistance and the chemistry of the cell but is usually

quoted between 2.5–3V for a layered oxide–graphite chemistry [6]. It is possible to over-discharge a cell below 0% SOC to an open circuit voltage of 0 V. This can be achieved through discharge via a resistor or external short circuit, care must be taken in performing this, as any remaining energy will be delivered as heat. If over-discharge is desired, it must be performed carefully and slowly, to prevent this heat build-up. It should be noted that over-discharging a cell to an end-of-discharge voltage of 0 V will also change the chemistry of the cell [7,8]. From our experience, copper from the current collectors in the battery tends to partially dissolve in the electrolyte when the battery is discharged to 0 V, this is due to the high potential observed by the anode at 0 V and oxidation of the copper [9]. After end of discharge voltage is reached, the cell is allowed to rest to open circuit voltage (OCV). Battery discharge can be accomplished by simply connecting a load across the battery terminals, this allows for potential energy collection and reuse. An alternative that can be used for cells (not modules and packs), is a salt-water electrochemical discharge method. This does not allow energy reclamation but can render the cells safe. A recent study analyzed this technique in some detail and concluded that several different aqueous salt solutions were capable of efficiently discharging the battery without damage [10]. In the case of damaged cells where discharge cannot be performed, more safety precautions will be necessary, often these are first "made safe" by short circuiting the cell through nail penetration or discharging in a brine solution before disassembly. This does however introduce greater potential for contamination of the materials streams during processing.

Once discharged, the battery is transferred to a controlled environment in order that it may be opened safely, because some chemicals inside the battery can react with water and with oxygen. This is often done in a glove box filled with argon [11,12]. Parts of the battery can then be separated. Systems for disassembling the battery have been described previously [13]. To date, in most cases these systems involve the separation of some battery parts manually, followed by shredding [4,14,15] or crushing [16,17] to attempt to recover useful materials. Due to the hazardous nature of the battery components it is essential that engineering controls such as glove boxes or fume hoods are used for handling battery materials. If the electrolyte is not removed from the reclaimed components, then hazardous materials can be released from them at a later stage in the process [18]. The electrolyte may be leached out of the components into water and procedures have been described for the optimization of this process, for example, using flotation tanks or including additives in the water for efficient leaching. [19–21] As was the case for the discharge process, the optimal procedures for battery dismantling may depend on the reason for which the battery is being dismantled; the requirements for an industrial recycling process may be different from the requirements of academic researchers who want to open the battery to characterize its components. Such studies can give important insight into how the material inside the battery changes during its useful lifetime [22,23].

An average of the chemical cell composition is given by Mossali et al., [24] however this was based upon an average of several cell types. We compare the several chemistries used in electric vehicle cells using BATPAC© Argonne National Labs, IL, USA. [25]–see Figure 1.

One of the principal challenges in Li-ion battery recycling is the sheer complexity of the battery itself. A typical battery is enclosed in a large pack housing, within which there is a number of modules (each containing several pouch cells), circuitry and the battery management system [30,31]. The exact layout of each of these components is different between manufacturers. Even at the pouch cell level, each cell contains many chemical components (outer pouch material, aluminum and copper sheets, anode and cathode material) and separating these is not a trivial problem. A particular challenge is presented by the anode and cathode materials, which consist of a mixture of various chemical components and require advanced chemical and physical methods, such as such as ultrahigh shear de-agglomeration, calcination and soxhlet extraction, froth flotation, selective leaching, direct regeneration and mechanochemical recovery, to be separated into 'pure' materials; their constituent materials parts with no or limited contamination. [32–38] The benefits of recycling and materials recovery are, however, substantial; in a truly circular economy, we should aim to recover and protect the critical materials contained in LIBs.

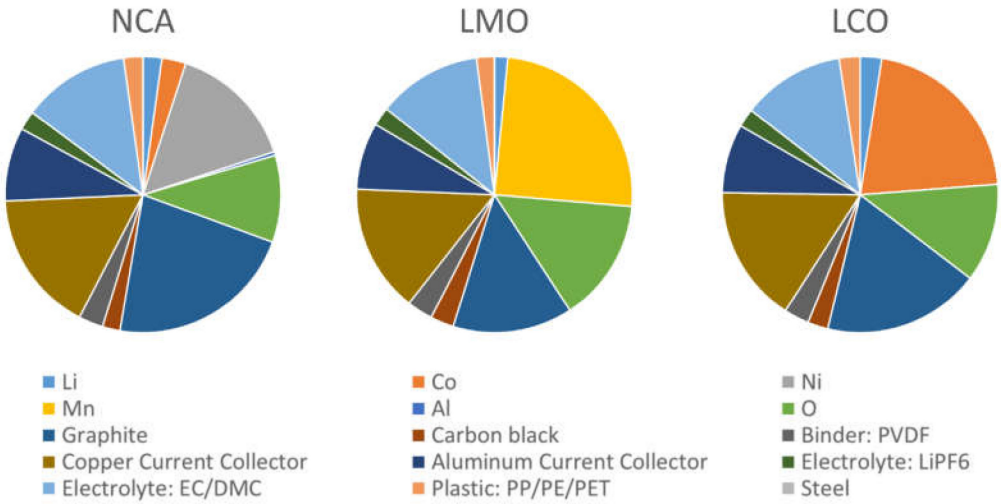

Figure 1. Percentage breakdown of components of a typical lithium ion battery (LIB) cell with different cathode materials $LiNi_{0.8}Co_{0.15}Al_{0.05}O_2$ (NCA), $LiMn_2O_4$ (LMO) and $LiCoO_2$ (LCO); identifying the key materials and critical and strategic materials [26,27] (values of each component given as a percentage by weight) [28]. As calculated for a prismatic cell using a basic cell model [29].

Figure 1 gives a visual representation of the materials present in three different prismatic LIB chemistries; $LiCoO_2$ (LCO), $LiMn_2O_4$ (LMO) and $LiNi_{0.8}Co_{0.15}Al_{0.05}O_2$ (NCA). In particular, it is imperative to find better ways to recover and re-use metals such as lithium and cobalt, due to the precarious nature of the global supply for these materials; over 50% of global lithium production is located in a few regions of South America [39], while over 60% of global cobalt production is located in one country, the Democratic Republic of the Congo [40,41].

There are concerted ongoing efforts in both academia and industry to improve the recovery levels of these critical materials but this is hindered by the fast moving nature of the industry. Recycling rates have been slow to increase, complicated by changing battery chemistries, changes in composition of materials and the lack of focus on prior material recovery stages.

As an alternative to current systems, this paper reports on work looking at dismantling and characterization of the components produced by hand dismantling systems. In order for disassembly processes to become part of the commercial recycling procedure for LIBs, there must be a potential for them to be automated, as has been discussed in the case of 'test' pouch cells [42]; we discuss how our findings can be used to identify where problems and opportunities may lie for automated disassembly of LIBs in the future, particularly in terms of the health and safety aspects of the cell opening procedures. The aim of this work was initially to produce high quality transition metal containing black mass for hydrometallurgical extraction for our project partners. However during the development of this disassembly process we also optimized the process to reclaim clean and pure materials waste streams from other components; separators, pouch material, current collectors. The composition, morphology and the change in properties are investigated for two types of different scrap cells—Quality Control (QC) Rejected and End of Life (EOL). The potential for re-use is discussed for the different components.

2. Materials and Method Development

The batteries used for this study were automotive pouch cells from a 1st-generation Nissan Leaf. The dimensions of each cell are 215 mm × 256 mm, each cell has a nominal voltage of 3.75 V. A single Nissan Leaf car contains 192 pouch cells (with 4 cells in each of 48 modules). Each pack stores an electrical energy of 24 kW.h. The cells have cathodes which are approximately 75% Lithium Manganese oxide spinel (LMO) with 25% Lithium Nickel Cobalt aluminum Oxide (NCA) on aluminum current collectors, this is similar to reported previously [43]. The mass ratio of LMO:NCA is calculated from the Inductively coupled plasma-optical emission spectrometry (ICP-OES) data as

shown in Supplementary S1. The anode is comprised of graphite anodes on copper current collectors. The electrolyte is $LiPF_6$ in an organic carbonate solvent. Our process is tailored for this battery with this chemistry. Although some aspects of the procedure are general, some will have to be tailored in order to be applicable to other battery chemistries in other car models.

The teardown procedure is as described in Figure 2. We begin with cells that have been discharged to a suitable OCV; for safety we check the voltage with a multimeter before beginning their disassembly. Then, in a fume hood we manually cut the pouch open with a ceramic scalpel; during this whole process, metallic tools are not used due to the risk of electrical discharge. When opening the cell with a scalpel, care is taken to avoid damaging personal protective equipment such as gloves. Incisions into the pouch cell are made around the edges of the cell, avoiding cutting the stack of electrodes and current collectors; this stack is then separated into individual components using tweezers. This minimizes contact between the gloves of the person carrying out the disassembly and the components that are impregnated with electrolyte. All tools are thoroughly cleaned after this procedure. We envisage that for a future automated process, the pouch incision could be made using a laser. Current investigations using laser-opening methods are ongoing; the operation of which is being optimized to reduce the heat transfer to the cell components whilst still cutting open the packaging, to ensure that thermal runaway does not occur. It is noted that the settings for a laminated aluminum pouch are different from a steel can. In addition, the laminated aluminum pouch is easily cut with a blade if necessary, whereas the steel can require greater power or energy to pierce. The pouch cell is the subject of this study. The cell components are physically separated into three groups; anode, cathode and 'other' materials. This physical separation minimizes the possibility of cross-contamination during further processing, this is currently by hand, however we foresee the ability to automate this process and some steps towards automatic separation have been reported [42,44,45]. It is noted however that upon opening of the cells, the $LiPF_6$ salt in the electrolyte can hydrolyze to produce HF and end of life cells may contain lithium dendrites. Therefore, processes need to be developed such that lithium dendrites are pacified (such as with CO_2 or water mist) and gaseous HF is not released to atmosphere. To remove the electrolyte and salt from the electrode, the three components are washed in separate solvent baths of isopropan-2-ol (IPA) in a fume cupboard at ambient temperature, before drying under vacuum, (the electrolyte remains in the bath). The procedure was attempted using a number of solvents, including acetone, diethyl carbonate, dimethyl carbonate and IPA. In some of these solvents, the electrode black mass delaminated from the metal films from the cell. IPA proved to be the most effective solvent for this process because it caused the least delamination and therefore was chosen as the washing solvent. In this case, we have not separated the electrolyte any further; the carbonates remain dissolved in the IPA or water and a white lithium containing precipitate starts to form over time. The aim of washing was to eliminate the possibility of HF forming from hydrolysis of the $LiPF_6$ salt during the further component processing and handling. After washing, the outer part of the pouch and the separator can be recycled. Then, the electrode 'black mass' can be separated from the copper and aluminum foil sheets. There are several ways of liberating the materials from the current collector; thermal liberation to break down the binder, [46,47] solvent delamination [21,48], physical methods such as ultrasonic and agitation. [49] Binder calcination forms HF due to decomposition of the PVDF and solvent delamination (in N-methyl Pyrrollidone (NMP)) produces a secondary waste which falls under current REACH regulations. [50] In this work, our focus was upon an environmentally conscious solution for scale-up to industry and therefore we chose to investigate a combination of ultrasonic delamination in a green solvent. Initially water and DMC were used with limited delamination effect; upon the addition of an acid (2 M HNO_3) we noticed significant delamination. From previous work on copper and aluminum corrosion, it is known that the mineral acids and alkali's will cause pitting of aluminum, particularly if the pH is below 4 or above 7 [51]. Copper will dissolve slowly into strong acids and in aqueous solutions above pH 3 will slowly oxidize. [52] Interestingly, previous work with oxalic acid shows a passivating effect on both aluminum [53] and copper [54]. We therefore chose oxalic acid, (pH 3), in water, as a greener delamination solvent alternative to NMP. Initially the

oxalic acid concentration was optimized for delamination of the QC rejected cells, where we observed the least damage and maximum delamination using weak organic solutions in an ultrasonic bath. Therefore, due to delamination efficiencies and secondary waste concerns we chose to concentrate and optimize the processes using oxalic acid in this study, greater efficiency or optimization may be possible utilizing alternatives. The black mass was extracted by sonication in a bath of oxalic acid at a respective optimized concentration for the copper and aluminum delamination process. It is possible to further reclaim the black mass components; active materials, conductive additive and binder (PVDF). These components are present in very small quantities (typically <10% by weight of the black mass). Heat treatments can break down and burn off the PVDF or binder [55], however we can only recover the active material components; graphite or the metal oxides. This process also delithiates the cathode materials [56] and also has the disadvantage of being quite energy-intensive. In this work we show as an example for the re-use case, materials which have been heat treated in this way. If we wish to recover all materials including the PVDF binder and to do this without such aggressive heating, it is necessary to consider a route that involves solvents to strip the binder out of the anode and cathode materials. We show as an example the possibility to remove the PVDF and carbon black from the black mass using NMP as a solvent. This however is not sustainable and further work for investigations of green solvents or other removal methods are required.

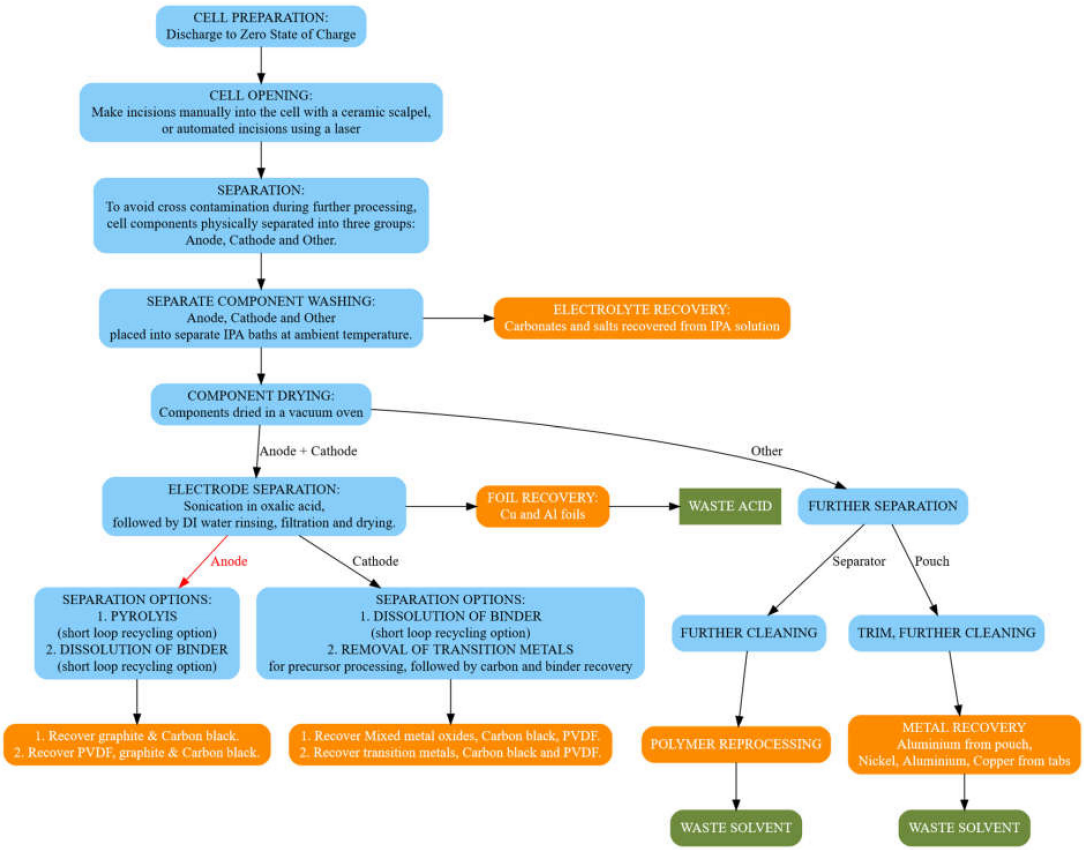

Figure 2. Schematic diagram describing our procedure for the disassembly of a Li-ion battery. Steps marked in blue are our procedure steps for each stage of the cell teardown. Boxes marked in orange represent the recovered materials. Boxes marked in green represent waste materials.

3. Experimental Details

Delamination—The anodic and cathodic "black mass" was separated from the copper and aluminum sheets present in the cell. The individual components were first washed in IPA or water (as above) and then dried for 24 h at 50–75 °C and 100 mBar. This was followed by a sonication process (40 Hz, 50 W) in a solution of oxalic acid, to remove the "black mass" from the metal foils. The anodic

"black mass" was separated from the copper foils in an oxalic acid bath concentration 0.02 M, for 30 min at ambient temperature; the cathodic "black mass" was separated from the aluminum foils in an oxalic acid bath at a concentration of 0.5 M, for 5 min at 50 °C. The subsequent composite black mass powders were dried under vacuum at 60 °C before further processing or re-use. The black mass materials can be deconstructed still further and the binder and conductive additives removed for example by either calcining or by chemical extraction methods, this is currently the subject of further study.

T-Peel tests were carried out on an Instron 30 kN test frame, in tension with a 500 N load cell and 1 kN wedge grips. Specimens were pre-loaded to 1.5 N to remove slack from the specimen and tested at 2 mm/min. Each specimen comprised of 2 adherends (25 mm × 120 mm) thermally bonded at one end. Specimens were bonded using the following parameters—temperature 160 °C, time 3 s, bond width 8 mm, pressure 40 kg·cm^{-2}. SEM analysis was carried out using a Hitachi Tabletop Microscope TM3030Plus (Hitachi High-Tech Corporation, Japan). For analysis of the pouch materials, each sample was coated in AuPd, sputtered at 80 mA for 80 s under vacuum (0.01 mBar).

ICP-OES analysis—The cathodes were characterized using ICP-OES (Optima 8000, Perkin Elmer Inc., Waltham, MA, USA). Prior to analysis, the cathodes were removed from a quality control reject cell, dried at 50–75 °C and 100 mBar overnight, washed in distilled water and dried again at 50–75 °C and 100 mBar overnight. Samples were cut from the electrode sheet and dissolved in in aqua regia.

The morphological analysis of the reclaimed material was conducted with the use of Scanning Electron Microscope (SEM) (JCM-7000, JEOL, 1930 Zaventem, Belgium) equipped with a secondary electron detector and under the acceleration voltage of 15 kV. The working distances applied for the SEM study were 6.0 mm and 10.0 mm with the latter applied for the EDS analysis as well.

Electrochemical testing of the black mass—The obtained black mass was ground, sieved and subsequently utilized for the slurry preparation. The anode ink contained—reclaimed graphite, carbon black (Super C65, Timcal, Imerys, 6804 Bironica, Switzerland), carboxymethyl cellulose (Bondwell BVH8, Ashland Industries Europe GMbH, Schaffhausen, Switzerland) and styrene butadiene 40 wt. % suspension in water (Zeon Europe GmbH, 40549 Düsseldorf, Germany) in a weight ratio—92:3:2:3. The cathode coating was prepared in a dry room (dew point of −50 °C) with the following constituents—reclaimed cathode material, carbon black (Super C65), PVDF (Solef® 5130, Solvay SA, 1120 Brussels, Belgium)–prepared as 8 wt.% solution in NMP with the weight ratios of the materials—94:3:3. Both slurries were prepared with the use of centrifugal mixer (Thinky ARE 250, Intertronics, Oxfordshire, UK,) and coated onto the aluminum and copper current collectors for positive and negative electrodes, respectively. The prepared coatings were dried on a hot plate at 50 °C–anode and 80 °C–cathode. Then, they were transferred to the vacuum oven (Binder) and dried overnight at 120 °C prior to the cell assembly.

Coin cells were assembled. The electrodes and separator were cut with a TOB electrode cutter, with the disc diameter adjusted to 14.8 mm, 15.0 mm and 16.0 mm for positive electrode, negative electrode and separator (Celgard 2325, Charlotte, NC, USA) respectively. Cells were constructed with a lithium metal counter electrode and filled with 70 µL electrolyte (1 M $LiPF_6$ in 3EC:7EMC PuriEl R&D261, Soulbrian, MI, USA). The assembled cells were tested using Bio-Logic, Seyssinet-Pariset, 38170 France, BCS cycler applying the following protocol for the anode half-cells—discharge at 0.05 C to 5 mV then charged back to 1.5 V at the same rate using constant current (CC) repeated twice. Followed by 0.2 C discharge and charge steps with the same voltage limits. The cathode half-cells were tested according to the following protocol—CC charge at 0.05 C to 4.2 V, CV step at 4.2 V and CC discharge to 2.8 V.

4. Results

We herein describe how each step of the procedure is to be followed safely and how each component may be reclaimed and possibly re-used.

4.1. Discharge and Cell Opening

Prior to opening the cells it is necessary to ensure that the Open Circuit Voltage (OCV) is low enough to commence a safe teardown. All relevant risk assessment and COSHH documents should be completed to ensure a safe scheme of work is followed due to the potentially toxic nature of these materials and the risk of sparking and/or fire. There is still some debate as to what the discharge level actually is on cell opening and how to accurately capture discharge data due to charge recovery effects. Furthermore, once discharged, there can be some minor charge recovery which may vary from battery to battery.

For the purposes of this study, batteries were provided to us already discharged to a suiTable SOC, in this case we discharged to 2.5 V cell voltage. At this level of discharge and as we are concerned with materials recovery rather than degradation analysis, we were able to open the pouch cells and separate the components in a fume cupboard (without an inert atmosphere) with no extreme adverse reactions. The fume hood must be well-ventilated to prevent release of any toxic materials into the working environment.

We examined cells in two different end states;

(1) Modules from EoL batteries that had previously been discharged to a low SOC (2.5 V) as recommended on a 2nd life data sheet [57]. Figure 3a is a photograph of one of these modules just as the outer module casing is opened. Inside are two plastic sheets (the blue layers in the photograph) and between these are 4 pouch cells, as shown in Figure 3b. Since the outer casing is mostly aluminum, it can be sent directly for metal recycling. The pouches are separated from the casing for further processing.

(2) Pouch cells that had been rejected as part of routine Quality Control (QC) procedures. Having been rejected during QC, these cells had never been placed in a module and were supplied as individual cells, discharged to 0 V. Such cells may be considered as part of the manufacturing waste associated with making LIBs. Figure 3c is a photograph of one of these cells. Figure 3d is a photograph of this cell after the pouch has been cut open to expose the layers of electrode materials in the pouch.

In both cases, before opening the actual pouches the external tabs on each cell were removed. The photograph in Figure 3c clearly shows these tabs, on the right-hand side of the photograph as viewed here. Note that the tabs are larger in the QC rejects, as they have never been welded and cut shorter during the process of being fitted into a module. These external tabs are made of Copper, coated in Nickel.

Once the tabs are removed, an incision is made through the outer wall of the pouch; this is done using a ceramic blade in order to prevent any potential risk of shock or short circuit between electrode layers (we envisage that in a future 'automated' version of this procedure, the incision could be made using a laser or automated knife). The pouch is slit open on three sides as shown in Figure 3d. The outer casing of the pouch is made of aluminum with a polymer coating, while inside each pouch there are multiple layers of copper, aluminum, anode and cathode 'black mass' materials and polypropylene (PP) separator layers. In addition, the electrode layers are suffused with the electrolyte solution.

Once the pouch is open, separate stacks are formed of copper foils (coated in anode black mass), aluminum foils (coated in cathode black mass) and the other components of the cell (aluminum pouch and PP separator. For the characterization of the cell components, these three stacks are kept separate in order to prevent cross-contamination. The following sections will deal with the separation and re-use of these components.

4.2. Materials Separation and Recovery

Figure 4 describes the average mass of material collection from the different components as the cell is split down into its various components, a complete analysis is shown in Table 1. A total of 80% and 77% of material is recovered from the QC rejects and EoL cells, respectively. The electrolyte is not currently being

reclaimed from the water and solvent waste and therefore this is the major loss in these numbers. These figures were obtained as an average from teardowns of three cells. From these data, we can conclude that the amounts of material recovered are similar at most stages of the process. Exceptions to this are the tabs (which are more readily recovered from QC reject cells, having not been welded into a module, as discussed above) and the electrode black mass, which is more heavily weighted towards the anodic black mass in the case of EoL cells. A number of factors could contribute to this result, including Li uptake into the anode, dendrite formation and Cu dissolution, in the case of EoL cells.

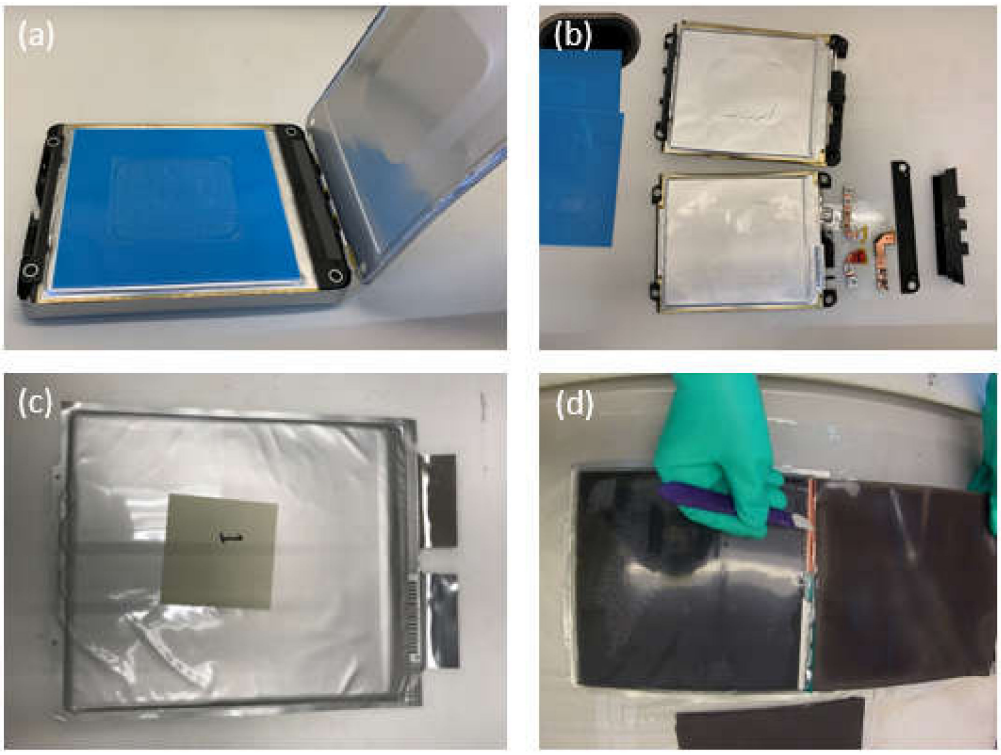

Figure 3. (**a**) Photograph of a module of an end of life (EoL) battery, straight after the casing is opened. (**b**) Photograph of the open module, showing the pouch cells inside. (**c**) Photograph of an individual Quality Control (QC) reject pouch cell. (**d**) Photograph of an open cell pouch, showing the layers of electrode materials within.

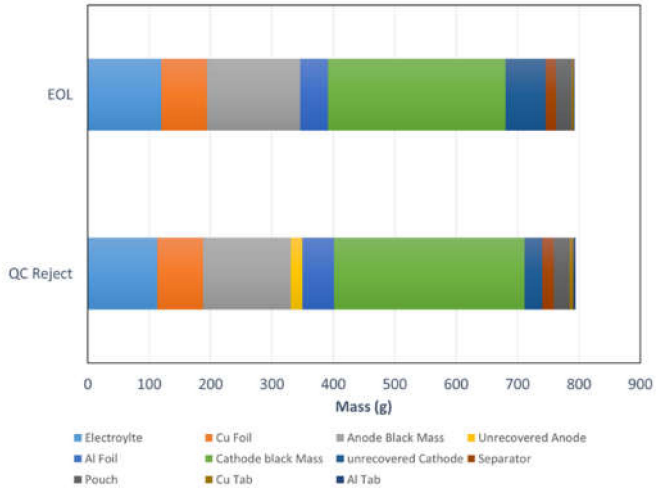

Figure 4. Shows the quantity of material reclaimed from the teardown methodology. Values are given for both QC reject and EoL cells. The values given are averaged over 3 cells.

Table 1. Summary of tear down and reclaimed masses of cell components from a QC rejected cell and EOL.

Cell, Components and Materials				QC Reject		EOL	
				Component Mass (g)		Component Mass (g)	
Full Cell				791.0(6)		795(1)	
Full Cell	Electrolyte			113(20)		120(1)	
	Electrodes	Anodes	Cu Foil	237(2)	74(2)	226.67(3)	74.6(2)
			Anode Black Mass		143(1)		152(2)
			Unrecovered Anode		19(1)		0.07(1)
		Cathodes	Al Foil	390(9)	51(2)	399.4(2)	44.41(5)
			Cathode black Mass		310(4)		290(1)
			Unrecovered Cathode		29.12		65.26
	Other	Plastics	Separator	44.0(4)	19.0(4)	42 (2)	17(1)
			Pouch		25.00(2)		25.1(2)
	Metals	Tabs	Cu Tab	1.01(1)	6.21(6)	5.23(6)	3.15(5)
			Al Tab		3.9(1)		2.08(2)

4.2.1. Electrodes: Current Collectors

The current collectors are easily reclaimed after the ultrasonic delamination process, the delamination is nearly 100% effective and little of the black mass is retained on the current collector. The current collectors which are obtained through purely removal of the electrode coatings using NMP solvent are shown in Figure 5. We can observe that for both the cathode and the anode significant indentations into the current collectors are observed. This is from the calendaring of the active material components onto the current collector in the manufacturing process. The image of the aluminum current collector (Figure 5b) has some remaining metal oxides which are clearly embedded into the current collector. The SEM images show insignificant changes between the reclaimed current collectors from solvent removal and the delamination process indicating minimal damage from the ultrasonic oxalic acid solution bath. The copper current collectors from the QC rejected cells have additional pitting due to the oxidation of the copper when discharged to 0 V, (Figure 5a). It should be noted the practice of taking QC rejected cells to 0 V is a safety measure to prevent these cells being used in any other application. The dissolution of the copper is confirmed by the presence of copper oxide in the cathode material as illustrated in the next section.

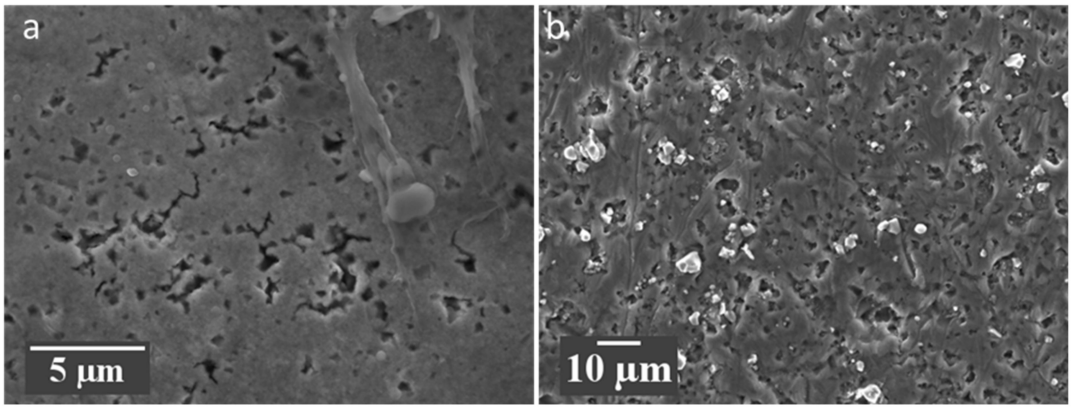

Figure 5. Scanning electron microscopy (SEM) images of copper (**a**) and aluminum (**b**) current collectors obtained from the QC reject electrodes.

4.2.2. Electrodes: Black Mass

The black mass separated from the metallic films by this process can then be filtered out of the oxalic acid bath and rinsed with water or with IPA. This black mass is comprised of the active component of the anode and cathode, with a conductive carbon and PVDF, the SEM images of the cathode from the QC rejected (a,b) and the EOL (c,d) cells are shown in Figure 6. The EDX analysis shows that the QC rejected cells have copper contamination from the discharge process to 0 V (Table S1.2). From the ICP-OES analysis (Table S1.1) the transition metal ratio Mn:Co:Ni is 74.7:2.8:22.5, which is similar to that observed by EDX. The undissolved content was calculated to be 6.7% by mass, this is due to the conductive carbon and PVDF content of the electrode coating. Indicating that there is approximately 93.3% current collector and active mass content for the cathode, which is reasonable. ICP-OES also showed 3.3% by weight of the total metal content. From EDX, the transition metal composition varied between the QC reject and the EOL, a greater percentage of cobalt was present in the EOL cell, possibly indicating low levels of manganese dissolution during the life-time of the cell. Ratios of Mn:Co:Ni are 74:3:23 and 73:6:22 for QC reject and EOL respectively. It should also be noted the Mn is preferentially leached by oxalic acid [58].

The anode black mass was analyzed using SEM-EDX, before and after washing in either IPA or in water. The elemental composition of the black mass varied across the electrode, therefore several elemental maps were taken over the electrode and averaged. Figure 7 shows the SEM images of the black mass from the QC reject and EOL cells. The elemental composition of and the morphology of the surface of the pieces of reclaimed electrode are slightly different depending where within the electrode they have come from. The sample shown in Figure 7a is the surface of the electrode, nearest the separator, whereas Figure 7b is that closest to the current collector. EDS mapping of the elements showed that fluorine concentrated in the spider-like covering shown in Figure 7b and initial XPS results indicate that this is from PVDF binder (Supplementary S2).

The EDS analysis of the black mass from the QC rejects and EOL cells was compared for samples which were not washed, washed in IPA and subsequently delaminated using oxalic acid solution (Table S2.1). We analyzed and compared the particles which were closest to the separator (S) and the current collector (C). The main elemental components in the EOL cell are carbon, fluorine, sulphur, phosphorous and aluminum, the samples obtained from close to the current collector contained a greater percentage of fluorine from the PVDF binder. The ratios of the washed electrodes are very similar to that of the unwashed electrodes, indicating very little change of the black mass composition upon washing. For the QC rejected cells, the black mass has a similar elemental composition to the EOL cells, except for copper being present. The quantity of copper was also variable depending upon whether the electrode was closest to the current collector or to the separator, as is expected the greater copper and fluorine percentage was observed closest to the current collector.

At this stage, we now have a separate stack of anode black mass and cathode black mass. The anode black mass contains graphite, carbon black, PVDF binder and other conductive additive. The cathode black mass contains Lithium Manganese Oxide (LMO) and Lithium Nickel Cobalt Aluminum Oxide (NCA powder), PVDF binder and conductive additive. Also, subsequent generations of automotive cells involve different chemistries, as well as binder polymer, so the separation process will need to be adapted for each model.

As an example; the SEM images shown in Figure 8a,b show large graphite particles (10–30 microns) connected by binder material. These particles are packed together fairly closely in the anode layer. After suspending some of this anode material in NMP (50 °C with ultra-sonication for 30 min) a suspension was formed; passing this liquid through a standard cellulose filter (Whatman grade 1) results in most (>90% of the material remaining on the filter. The SEM images in Figure 8c,d show discrete separated graphite particles resulting from graphite reclamation via this route. The PVDF binder then remains in the solvent used to strip it from the graphite and can be recovered either by evaporation of the solvent or by addition of a non-solvent to remove it from the solution. This process however uses the solvent NMP and therefore alternative routes are required to ensure a more sustainable process.

The exact processes used to separate the electrode components will depend on the specific requirements for the reclaimed material. From this process, the copper and aluminum metal sheets can be cleanly recovered for potential reuse. The waste acid produced in the oxalic acid bath may be contaminated with heavy metals or particulates and will require further treatment for recovery. The cathodic black mass produces a mixed metal oxide material which can be sent for hydrothermal or pyro metallurgical extraction but still contains the PVDF and carbon black at this stage and the anodic black mass contains mainly graphite with PVDF and carbon black. We have shown the potential for future post processing, such as solvent extraction of the PVDF and the carbon black or potentially heat treatments. Significantly more work is required to understand the effects of the post processing upon the active materials and hence the potential for re-use. For the purposes of demonstration of black-mass re-use (Section 4), we have utilized heat treatment for post-processing the black mass after reclamation, this is because the as reclaimed materials did not perform. Heat treatments have safety implications as HF is produced as the PVDF decomposes.

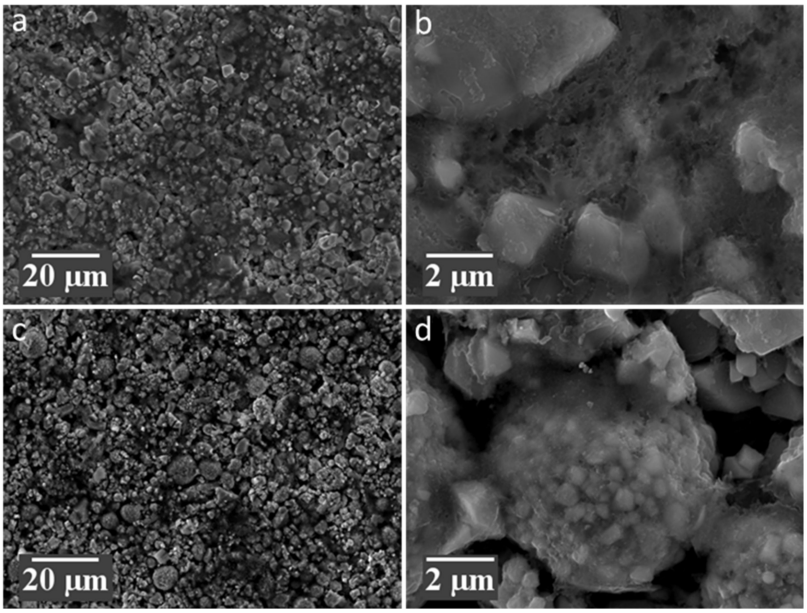

Figure 6. SEM images of the reclaimed cathode black mass for (**a**,**b**) QC rejected cells and (**c**,**d**) end of life cells.

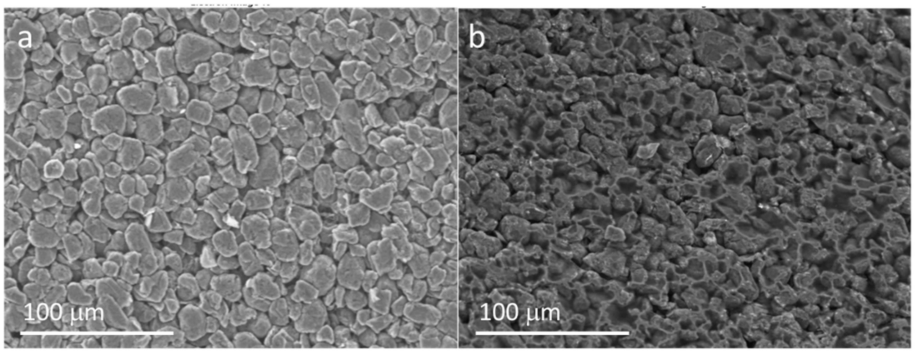

Figure 7. SEM images of anode black mass for (**a**) QC rejected cell and (**b**) EOL cell. Both electrodes have been washed in IPA (**a**) is the surface of the electrode nearest the separator and (**b**) is towards the current collector.

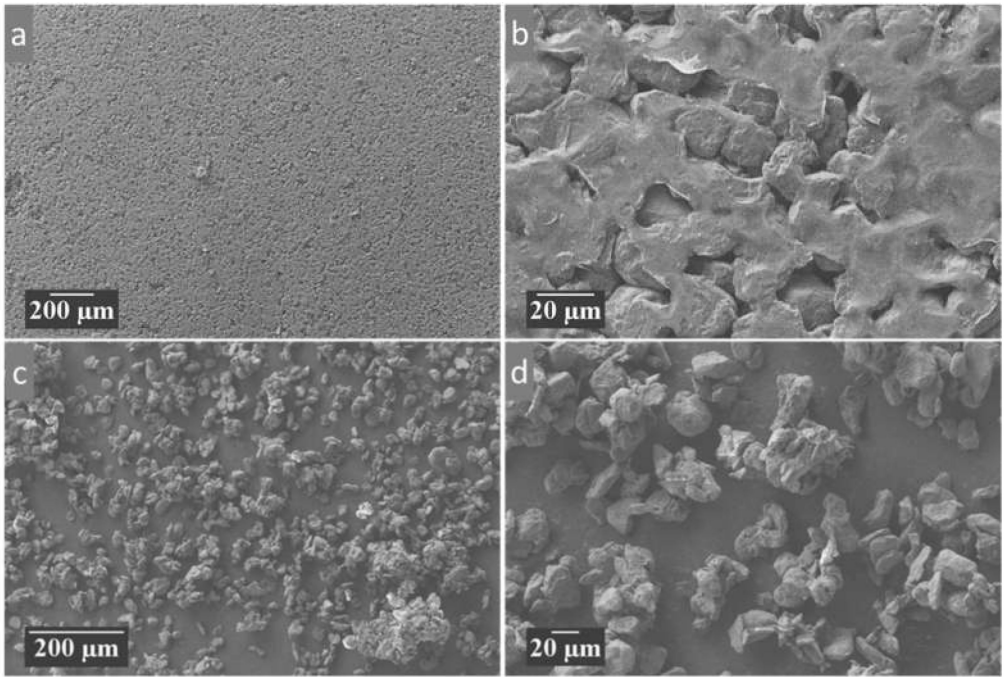

Figure 8. SEM images showing (**a**), (**b**) the anode material after being separated from the copper film (**c**), (**d**) graphite particles from the anode, after the binder is removed by dissolving in NMP (N-methyl Pyrrollidone) followed by filtration.

4.2.3. Electrolyte

The procedure to be followed in order to collect and characterize the electrolyte depends on the aim of the cell teardown. If the aim is simply to collect the electrodes for recycling and in this case the cathodic black mass for hydrometallurgical processing, it may not be necessary for separation of the solvent and electrolyte salt. Here we have not reclaimed the solvent or the salt from the washings. The quantity of solvent and salt has been calculated from the difference in the weights of the total cell and the disassembled and washed components. However, the solvent and the salt can be reclaimed from the washings through precipitation and solvent evaporation. The salt however will not be collected as $LiPF_6$ as it is unstable in water and LiF will precipitate over time as the $LiPF_6$ reacts [59,60].

4.2.4. Outer Pouch

The outer pouch, separator and trim materials make up roughly 7% by weight of a dismantled battery cell. This particular waste stream is, however, of considerably lower economical value than the critical materials (particularly metals) present in the electrodes and electrolyte. Once collected, the pouch is placed in a water bath and subsequently tested for re-use/recycling.

The unused pouches in this system are made of aluminum covered by a polymer coating; the inner coating is polypropylene (PP) while the outer coating contains polyethylene terephthalate (PET) and nylon 6 (PA6). We will use the as-supplied pouches as a 'baseline,' to which we can compare the reclaimed pouches. Figure 9 presents SEM images from the inner surface of the 'baseline' pouch material compared to that of a reclaimed pouch from a QC reject cell.

T-Peel tests were carried out on 14 specimens, using a method based on ISO 11339. Each specimen comprised 2 adherends (25 mm × 120 mm) thermally bonded at one end. There were 5 pristine pouch material specimens and 9 specimens made from reclaimed pouch (from a QC reject cell). Figure 10a gives example load vs extension curves for one example of a "baseline" pouch and a "reclaimed" pouch. In the 0–5 mm extension regime, both curves show an initial maximum load; between 10–15 mm the load variation is flatter. Figure 10b gives average results across all samples tested, for the initial peak load, the maximum load obtained and the mean load seen across the "flatter" 5–15 mm region. It is

clear that the reclaimed pouches retain much of their mechanical strength; while there is some decrease in the initial peak load and overall maximum load, the load variation across the 5–15 mm region has not changed significantly. Therefore, it appears likely that pouch materials could be reused (in smaller format sizes) if the weldability of the reused PP can be determined to be safe. Alternatively, it may be beneficial to re-use the pouch material in a less hazardous environment as part of an alternative supply chain.

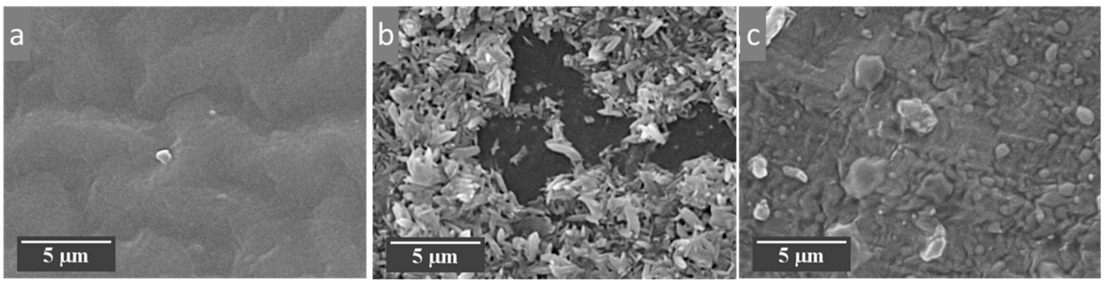

Figure 9. SEM images of the inner surface of (**a**) a "pristine" pouch, compared to (**b**) and (**c**) a surface from a reclaimed pouch (from a QC reject cell) that has been washed and dried. It is clear that some modification of the surface has occurred.

4.2.5. Separator Films

The separator is a porous polypropylene (PP) film held between the two layers of black mass forming the cathode and anode. It is peeled away from the layers of black mass during the cell disassembly stage.

In order to investigate the contamination of the separator, we cleaned pieces of separator by ultra-sonication in solvents for 30 min (ultrasound at 50 W and 40 KHz was used; the ultrasound bath was held at 50 °C during this time). The separator films were then dried and re-weighed. The difference in mass between the initially reclaimed separator and the separator after washing and drying is shown in Figure 11. In all of these solvents, a significant decrease in mass was seen after the washing process; we conclude that the solvents abstracted a significant amount of impurity from each film.

In addition, we note that the separator films were very weak and easily tore during the battery dismantling process. It therefore seems unlikely that they can be re-used as separator films. PP is a commonly recycled polymer, however and (depending on the cleaning procedures) it could be recycled in products requiring lower grade PP.

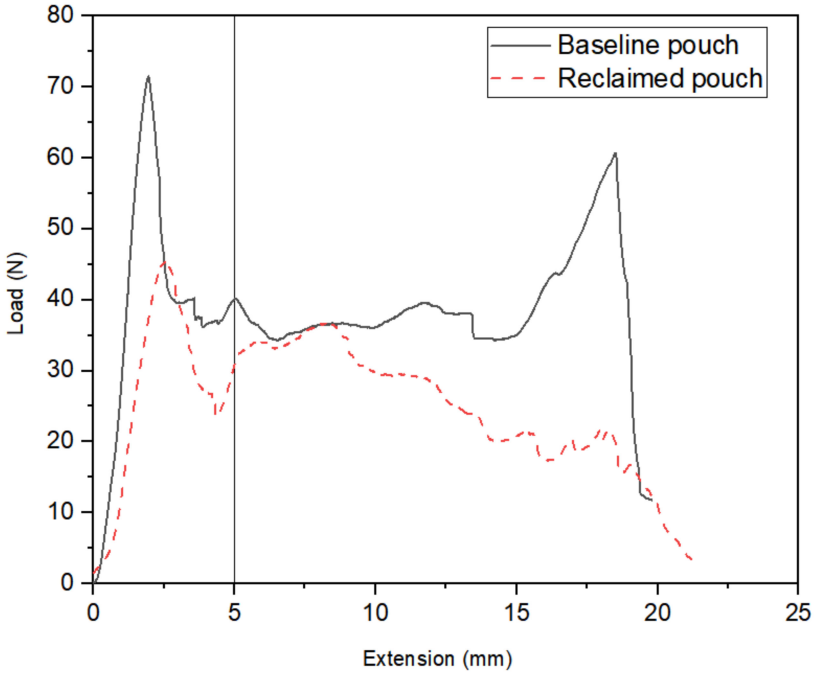

(**a**)

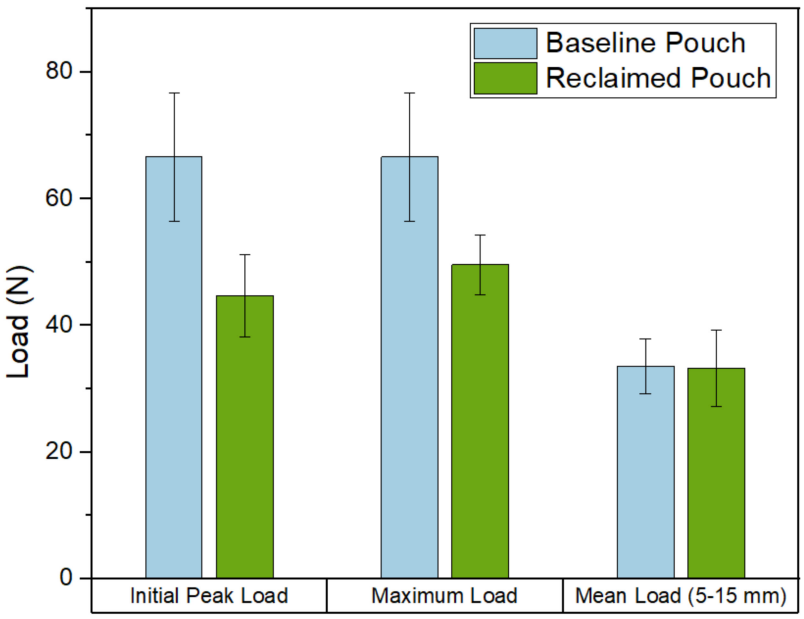

(**b**)

Figure 10. Graphs to show load vs extension curves for a number of pouch specimens. (**a**) Gives an example load vs extension graph for a baseline pouch compared to a reclaimed pouch. We see an initial peak load below 5 mm and then the graph appears flatter between 5–15 mm. (**b**) compares the average peak load, maximum load and mean load over a number of baseline and reclaimed pouches.

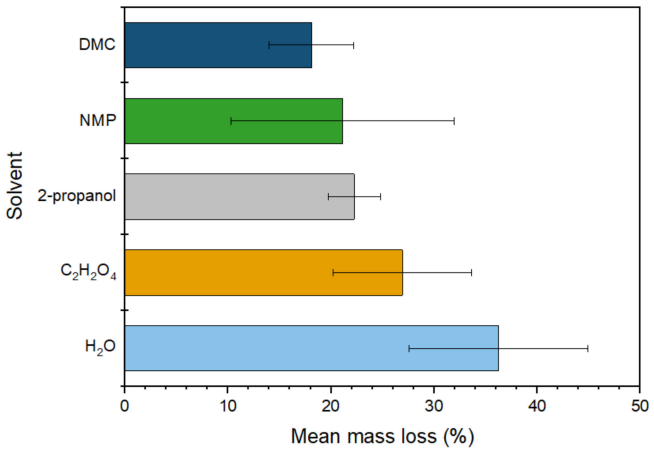

Figure 11. Mass loss of the separator on washing with various solvents (DMC, NMP, IPA, oxalic acid and water).

5. Reuse and Recycling of the Components

After reclamation we must consider the re-use cases for the cell components that we have extracted. We consider the current collectors, separator, pouch and black mass.

5.1. Pouch Materials

Used pouch material still has comparable mechanical strength to pristine pouch material. T-Peel tests show a slight decrease in the initial peak load and overall maximum load but the results are broadly comparable. If it can be demonstrated that the weldability of the pouch material is suitable, there is potential for used pouch material to be reused in new pouch cells, albeit of a smaller format. Used pouch material could also find applications in less hazardous environments if mechanical strength is paramount.

5.2. Current Collectors

The Aluminum current collector is affected by the processing and is more delicate than the copper. Figure 5 shows SEM images of current collectors from an uncycled (QC reject) cell, with the electrode coating removed using NMP. The current collectors are pitted despite not being processed using ultrasound. The copper current collector is affected by the state of charge it is stored at and ICP-OES and EDX data in Supplementary Data Tables S1.1 and S1.2 show Cu contamination in the cathode and anode black mass which is attributed to the dissolution of copper in the overdischarge process applied to these cells. The pitting and possible dissolution further weaken the foils, making reuse in a new cell difficult. Large scale electrode manufacture prints onto long rolls of foil which are cut into discrete foils after printing. Laboratory scale operations can use draw down coaters for individual foils. Recovering Al in the metallic form allows it to be recycled. Recycling Al saves 95% of the energy invested in primary production of Al [61].

5.3. Black Mass

The black mass for the negative and positive electrodes were collected separately, Cathode Black Mass was analyzed using SEM-EDS, compared to the untreated electrode from supplementary data Table S1.2 and is shown in Table 2. These results show a similar Ni:Mn and Ni:Co ratio to the starting material, although the Co content of the end of life material has decreased over the lifetime of the cell.

Graphite anode black mass content was analyzed to be variable as shown by XPS and EDX (Table S2.1) was dependent upon the position in the electrode, however if we assume the total carbon is an average of the surfaces, we observe 91.9% carbon by weight for the end of life and 91.95% by

weight for the QC rejected cell. The major additional content was from fluorine and in the case of the QC rejected copper. It should be noted that the lithium content was not possible to analyze.

Table 2. Metal Ratios of an untreated electrode (Data from Table S2.1) and two electrodes treated with the ultrasonic separation technique.

Metal Ratios	Untreated Electrode	Ultrasonicated QC Reject	Ultrasonicated EOL
Ni:Mn	0.30	0.31	0.30
Ni:Co	8.1	7.8	3.9
Co:Mn	0.04	0.04	0.08

To investigate the re-use case for the anode and cathode, the respective black mass was made directly into an electrode after drying (Figure 12). Initial results were poor where both anode and cathode exhibited high polarization and low capacities. In the case of the cathodic black mass, the processing in oxalic acid solution has affected the reclaimed cathode. Although not observable from X-ray diffraction measurements, it is likely that the surface of the materials have reacted to form carbonates, hydroxides or oxalates, which will form a resistive coating. We therefore investigated post treatment of the black mass. The cathode black mass was heat treated at 300 °C for 4 h. whereas, the anode black mass was heat treated at 600 °C for 2 h.

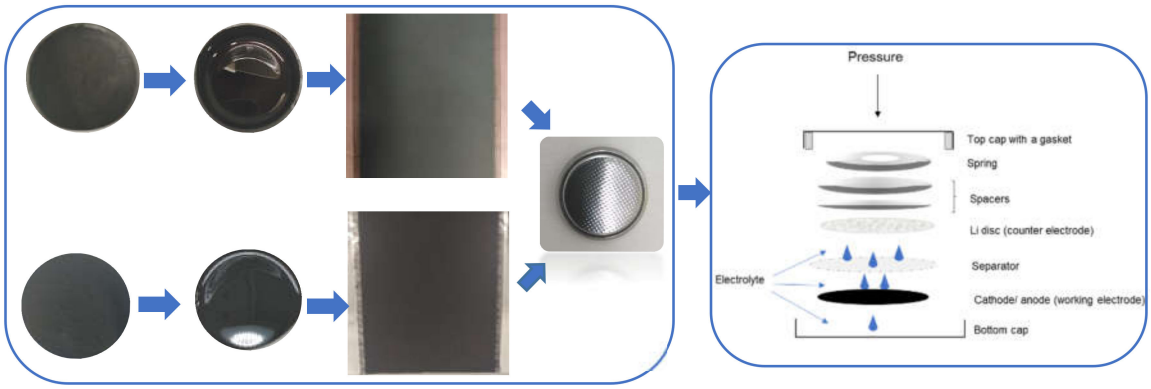

Figure 12. Anode and cathode coating preparation from the reclaimed material, top diagram presents anode, bottom cathode process steps: reclaimed active material, mixed slurry, electrode coating and coin cell.

The obtained results from the formation cycles of the half-cells testing are presented in Figure 13. The measured specific capacities of the graphite are 360 mAh·g^{-1} and 370 mAh·g^{-1} for the material reclaimed from QC reject and EoL cells, respectively. The specific capacity of the reclaimed cathode material is of 66.2 mAh·g^{-1} for the cathode black mass. The first cycle efficiencies for all the half-cells were measured to be above 90%. From the results shown from the EOL cathode material, we can see that the water and oxalic acid negatively affects the performance of the cathode. In order to "reclaim" any capacity from the materials they must first be heat-treated. Even with this heat treatment, the specific capacities are still significantly lower than we would expect. This indicates a likely loss of lithium during the reclamation process and relithiation steps require investigating for short loop recycling. If we consider however the black mass for hydrometallurgical and pyro metallurgical processes, there is very little loss of transition metal during the reclamation processes. The cathodic black mass waste stream has an extremely high purity of transition metal Mn:Ni:Co which can be leached and separated for synthesizing into a new cathode material or utilized in other industries. Cobalt is used in animal feeds and pigments, manganese has applications in steel and metallurgical

alloys, primary alkaline batteries, chemical feed for water purification and treat waste water, Nickel is used in metallurgical alloys for example in coins and turbine blades.

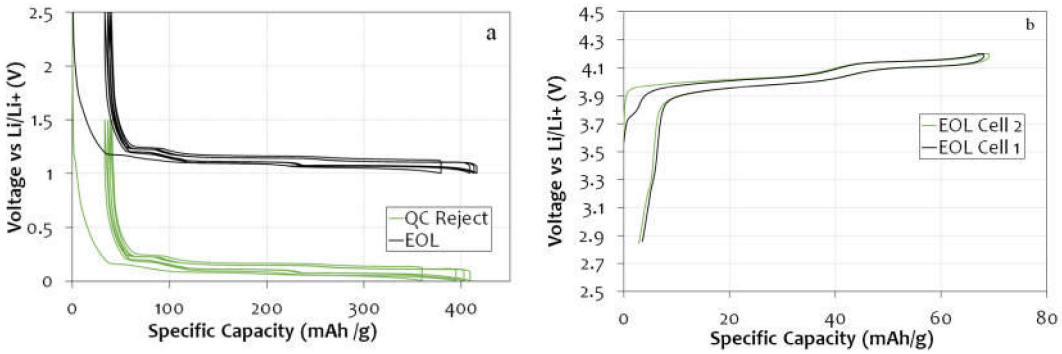

Figure 13. Formation cycle of the (**a**) anodes half-cells from QC reject and end of life anodes (**b**) and two cathode half-cells for end of life cathode after heat treatment of the reclaimed black mass.

From the above analysis of the re-use of the components, there is a possibility to re-use each component apart from the electrolyte. Each component has been compromised in some way from the use, disassembly and reclamation of the components. The current collectors are dented and pitted. We expect that if re-used the level of contact between the current collector and active components reduced, which will increase the resistance. The separator and pouch material have both been damaged in the cell and the strength reduced. The black mass requires post processing and heat treatment before it can be used. We demonstrate that we can short loop recycle the graphite and we obtain good specific capacities during low rate cycling, the cathodic black mass requires further re-lithiation, we observe useable capacities but with a large resistance. However, the cathodic black mass is suitable for further hydrometallurgical separation and is present in a very pure materials stream for reclamation.

6. Conclusions

As discussed above, there are significant challenges inherent in the recycling of Li-ion batteries, not least of which is the variety of different chemistries in use for the cathode and anode materials. Any one approach cannot be completely general and must be adapted for the particular system being used. However, valuable insight is gained by dismantling a battery of one type and some parts of the procedure can be generalized. This is part of the hierarchy of recycling, and we have investigated the potential for re-use or remanufacturing with materials, as we further refine the waste streams. The work was originally focused upon reclamation of pure cathodic black mass waste stream for further hydrometallurgical extraction of the transition metal components, and subsequently the disassembly route developed to reclaim most of the component parts in decontaminated waste streams. We have developed a methodology with a sustainable disassembly route in mind, using sustainable solvents, low cost routes and no toxic chemicals. We also discuss the safety aspects of each process, and the methodology we have adopted to ensure chemical and electrical safety.

The principal limitation of this approach is that it is rather labor-intensive, as it requires a person to manually make incisions in the cell and separate the internal components. However, some steps of the procedure could be automated, such as the opening of the pouch in order to separate the pouch components into separate stacks. Automation of the procedure would allow this process to be scaled up. The bottle necks in the automation are in cell opening and component separation. In both of these steps consideration around the types of chemicals potentially formed during the process or with exposure to air is required. In addition, the components material composition for the equipment needs consideration to ensure no corrosion of the parts. In addition, there are many types of cells; cylindrical, pouch and prismatic which are constructed in different manners, with different materials and joining mechanisms. Intelligent designs of equipment and identification tools will be required in order to identify the different cell types and therefore knowledge upon how to dismantle them.

In this article, we have demonstrated a workable method for the safe dismantling of pouch cells and have compared differences in method for the dismantling of EoL cells and QC reject cells. This "disassembly" approach allows us to recover most of the valuable materials present in each cell and to separate them into material types with greater purity than is usually possible using conventional methods that involve shredding the battery. This approach, then, has a considerable environmental benefit, as it can allow for potential re-use of some components and recovery of others for recycling.

In terms of the materials that are usefully recovered using this process, we straightforwardly obtain a significant quantity of aluminum and copper in the form of the current collectors, polymer from the separator films and the 'black mass' from the electrodes. Further processing is required in order to extract useful materials from the black mass. For some of the low-concentration chemical components of the black mass, it may be uneconomic to separate them completely and a short-loop recycling process may be more appropriate; this will be the subject of a future article. The polymer separators are unsuitable for simple re-use but have the potential to be recycled to form lower-grade polymer materials.

It is apparent that not all the components can be re-used, and if they are re-used they may have life-time and contamination issues. We have demonstrated the electrochemical performance of the anodic and cathodic black mass from the reclaimed and reprocessed materials, and show that the graphite can be short loop recycled, but the reclaimed cathode requires further relithiation. This is part of the circular economy for battery materials; some components can be re-used at different points of reclamation and some require remanufacturing. The ability to produce a completely recycled cell from the reclaimed components is unrealistic at present, but it may be possible to remanufacture the component parts from the reclaimed materials to produce a recycled cell. This is a great example of the circular economy picture for lithium ion battery recycling.

Supplementary Materials: The following are available online at http://www.mdpi.com/2075-4701/10/6/773/s1, Supplementary S1: Analysis of Cathode Black Mass; Supplementary S2: Analysis of Anode Black Mass. Figure S1. 1 EDX mapping analysis showing distribution of the elements (a), the transition metals Mn (b) and Ni (c) in the SEM images, there appear to be two separate phases the first is Mn rich, the second is Ni rich. Table S1. 1 ICP-OES analysis of the extracted cathode electrode, washed with distilled water, not delaminated. Table S1. 2. EDX analysis of the elemental composition of the QC reject and EOL after washing and delamination. Figure S2. 1 SEM (a) and EDS elemental mapping (b) of QC rejected anode, showing copper contamination throughout the electrode. Figure S2. 2 SEM (a) and EDS elemental mapping (b) of EOL cell, showing carbon particles and patches of high fluorine content due to the PVDF binder. Figure S2. 3 XPS analysis of the surface of the QC rejected anode black mass, and the fluorine analysis. Table S2. 1 Elemental composition analysed by EDX of the anode black mass with different treatments and positions within the cell, C–closest to current collector, S–closest to separator.

Author Contributions: Conceptualization, E.K. and V.G.; methodology, D.G., R.S., B.M., J.M.; investigation, D.G., R.S., J.M., B.M.; writing-original draft preparation, J.M., E.K, R.S. writing-review and editing, D.G., R.S., B.M., V.G., E.K.; supervision, E.K. and V.G.; funding acquisition, E.K. and V.G.; project administration, E.K. and V.G. All authors have read and agreed to the published version of the manuscript.

Funding: We acknowledge funding from UKRI project "Reclamation and Re-manufacture of lithium ion batteries," reference number 104425, and Faraday Institution ReLIB FIRG005 and FIRG006.

Acknowledgments: We would like to acknowledge the help of Marc Walker and the use of the XPS facilities at the Warwick Photoemission Facility (University of Warwick). We acknowledge Marny Bharndal (University of Warwick) for assistance with the T-Peel tests. We also acknowledge the ReLIB team at Birmingham, particularly Anton Zorin, Newcastle, and Leicester for helpful discussions and advice.

Conflicts of Interest: The authors declare no conflict of interest. The funders had no role in the design of the study; in the collection, analyses or interpretation of data; in the writing of the manuscript or in the decision to publish the results.

References

1. Heelan, J.; Gratz, E.; Zheng, Z.; Wang, Q.; Chen, M.; Apelian, D.; Wang, Y. Current and Prospective Li-Ion Battery Recycling and Recovery Processes. *JOM* **2016**, *68*, 2632–2638.
2. Velázquez-Martínez, O.; Valio, J.; Santasalo-Aarnio, A.; Reuter, M.; Serna-Guerrero, R. A Critical Review of Lithium-Ion Battery Recycling Processes from a Circular Economy Perspective. *Batteries* **2019**, *5*, 68. [CrossRef]
3. Tarascon, J.M.; Armand, M. Issues and challenges facing rechargeable lithium batteries. *Nature* **2001**, *414*, 359–367.
4. Harper, G.; Sommerville, R.; Kendrick, E.; Driscoll, L.; Slater, P.; Stolkin, R.; Walton, A.; Christensen, P.; Heidrich, O.; Lambert, S.; et al. Recycling lithium-ion batteries from electric vehicles. *Nature* **2019**, *575*, 75–86. [CrossRef]
5. Waldmann, T.; Iturrondobeitia, A.; Kasper, M.; Ghanbari, N.; Aguesse, F.; Bekaert, E.; Daniel, L.; Genies, S.; Gordon, I.J.; Löble, M.W.; et al. Review—Post-mortem analysis of aged lithium-ion batteries: Disassembly methodology and physico-chemical analysis techniques. *J. Electrochem. Soc.* **2016**, *163*, A2149–A2164. [CrossRef]
6. Kobayashi, Y.; Kobayashi, T.; Shono, K.; Ohno, Y.; Mita, Y.; Miyashiro, H. Decrease in Capacity in Mn-Based/Graphite Commercial Lithium-Ion Batteries. *J. Electrochem. Soc.* **2013**, *160*, A1181–A1186. [CrossRef]
7. Golubkov, A.W.; Scheikl, S.; Planteu, R.; Voitic, G.; Wiltsche, H.; Stangl, C.; Fauler, G.; Thaler, A.; Hacker, V. Thermal runaway of commercial 18650 Li-ion batteries with LFP and NCA cathodes - Impact of state of charge and overcharge. *RSC Adv.* **2015**, *5*, 57171–57186. [CrossRef]
8. Sonoc, A.; Jeswiet, J.; Soo, V.K. Opportunities to improve recycling of automotive lithium ion batteries. *Procedia CIRP* **2015**, *29*, 752–757.
9. Hendricks, C.E.; Mansour, A.N.; Fuentevilla, D.A.; Waller, G.H.; Ko, J.K.; Pecht, M.G. Copper Dissolution in Overdischarged Lithium-ion Cells: X-ray Photoelectron Spectroscopy and X-ray Absorption Fine Structure Analysis. *J. Electrochem. Soc.* **2020**, *167*, 090501. [CrossRef]
10. Shaw-Stewart, J.; Alvarez-Reguera, A.; Greszta, A.; Marco, J.; Masood, M.; Sommerville, R.; Kendrick, E. Aqueous solution discharge of cylindrical lithium-ion cells. *Sustain. Mater. Technol.* **2019**, *22*, e00110. [CrossRef]
11. Aurbach, D.; Markovsky, B.; Rodkin, A.; Cojocaru, M.; Levi, E.; Kim, H.J. An analysis of rechargeable lithium-ion batteries after prolonged cycling. *Electrochim. Acta* **2002**, *47*, 1899–1911. [CrossRef]
12. Williard, N.; Sood, B.; Osterman, M.; Pecht, M. Disassembly methodology for conducting failure analysis on lithium-ion batteries. *J. Mater. Sci. Mater. Electron.* **2011**, *22*, 1616–1630.
13. Wegener, K.; Andrew, S.; Raatz, A.; Dröder, K.; Herrmann, C. Disassembly of electric vehicle batteries using the example of the Audi Q5 hybrid system. *Procedia CIRP* **2014**, *23*, 155–160.
14. Wang, X.; Gaustad, G.; Babbitt, C.W. Targeting high value metals in lithium-ion battery recycling via shredding and size-based separation. *Waste Manag.* **2016**, *51*, 204–213. [CrossRef]
15. Sloop, S.; Crandon, L.; Allen, M.; Koetje, K.; Reed, L.; Gaines, L.; Sirisaksoontorn, W.; Lerner, M. A direct recycling case study from a lithium-ion battery recall. *Sustain. Mater. Technol.* **2020**, *25*. [CrossRef]
16. Diekmann, J. Ecological recycling of lithium-ion batteries from electric vehicles with focus on mechanical processes. *J. Electrochem. Soc.* **2017**, *164*, A6184–A6191.
17. Smith, W.N.; Swoffer, S. Recovery of lithium ion batteries. U.S. Patent 8616475B1, 31 December 2013.
18. Grützke, M.; Krüger, S.; Kraft, V.; Vortmann, B.; Rothermel, S.; Winter, M.; Nowak, S. Investigation of the Storage Behavior of Shredded Lithium-Ion Batteries from Electric Vehicles for Recycling Purposes. *ChemSusChem* **2015**, *8*, 3433–3438. [CrossRef]
19. Marinos, D.; Mishra, B. An Approach to Processing of Lithium-Ion Batteries for the Zero-Waste Recovery of Materials. *J. Sustain. Metall.* **2015**, *1*, 263–274. [CrossRef]
20. Wang, M.M.; Zhang, C.C.; Zhang, F.S. Recycling of spent lithium-ion battery with polyvinyl chloride by mechanochemical process. *Waste Manag.* **2017**, *67*, 232–239. [CrossRef]
21. Meshram, P.; Pandey, B.D.; Mankhand, T.R. Extraction of lithium from primary and secondary sources by pre-treatment, leaching and separation: a comprehensive review. *Hydrometallurgy* **2014**, *150*, 192–208.

22. Kovachev, G.; Schröttner, H.; Gstrein, G.; Aiello, L.; Hanzu, I.; Wilkening, H.M.R.; Foitzik, A.; Wellm, M.; Sinz, W.; Ellersdorfer, C. Analytical Dissection of an Automotive Li-Ion Pouch Cell. *Batteries* **2019**, *5*, 67. [CrossRef]
23. Qian, D.; Ma, C.; More, K.L.; Meng, Y.S.; Chi, M. Advanced analytical electron microscopy for lithium-ion batteries. *NPG Asia Mater.* **2015**, 7.
24. Mossali, E.; Picone, N.; Gentilini, L.; Rodrìguez, O.; Pérez, J.M.; Colledani, M. Lithium-ion batteries towards circular economy: A literature review of opportunities and issues of recycling treatments. *J. Environ. Manage.* **2020**, *264*, 110500. [CrossRef]
25. BatPaC Model Software|Argonne National Laboratory. Available online: www.anl.gov/cse/batpac-model-software (accessed on 24 November 2019).
26. *Study on the Review of the List of Critical Raw Materials—Critical Raw Materials Factsheets*; EU Publications, European Commission: Brussels, Belgium, 2017; pp. 1–93.
27. Fortier, S.M.; Nassar, N.T.; Lederer, G.W.; Brainard, J.; Gambogi, J.; McCullough, E.A. *Draft Critical Mineral List—Summary of Methodology and Background Information—U.S. Geological Survey Technical Input Document in Response to Secretarial Order No. 3359*; U.S. Geological Survey: Reston, VA, USA, 2018. [CrossRef]
28. Gaines, L.; Cuenca, R. *Costs of Lithium-Ion Batteries for Vehicles*; U.S. Department of Energy-Office of Scientific and Technical Information: Argonne, IL, USA, 2000.
29. Dai, Q.; Spangenberger, J.; Ahmed, S.; Gaines, L.; Kelly, J.C.; Wang, M. *EverBatt: A Closed-loop Battery Recycling Cost and Environmental Impacts Model*; Department of Energy-Office of Scientific and Technical Information: Argonne, IL, USA, 2019.
30. Gaines, L. Lithium-ion battery recycling processes: research towards a sustainable course. *Sustain. Mater. Technol.* **2018**, *17*, e00068.
31. Gaines, L. The future of automotive lithium-ion battery recycling: charting a sustainable course. *Sustain. Mater. Technol.* **2014**, *1–2*, 2–7.
32. Zhan, R.; Payne, T.; Leftwich, T.; Perrine, K.; Pan, L. De-agglomeration of cathode composites for direct recycling of Li-ion batteries. *Waste Manag.* **2020**, *105*, 39–48. [CrossRef]
33. Paulino, J.F.; Busnardo, N.G.; Afonso, J.C. Recovery of valuable elements from spent Li-batteries. *J. Hazard. Mater.* **2008**, *150*, 843–849.
34. Zhan, R.; Oldenburg, Z.; Pan, L. Recovery of active cathode materials from lithium-ion batteries using froth flotation. *Sustain. Mater. Technol.* **2018**, *17*, e00062.
35. Gao, W. Lithium carbonate recovery from cathode scrap of spent lithium-ion battery: a closed-loop process. *Environ. Sci. Technol.* **2017**, *51*, 1662–1669.
36. Li, X.; Zhang, J.; Song, D.; Song, J.; Zhang, L. Direct regeneration of recycled cathode material mixture from scrapped LiFePO4 batteries. *J. Power Sources* **2017**, *345*, 78–84.
37. Dolotko, O.; Hlova, I.Z.; Mudryk, Y.; Gupta, S.; Balema, V.P. Mechanochemical recovery of Co and Li from LCO cathode of lithium-ion battery. *J. Alloys Compd.* **2020**, *824*. [CrossRef]
38. Lestriez, B. Functions of polymers in composite electrodes of lithium ion batteries. *Comptes Rendus Chim.* **2010**, *13*, 1341–1350.
39. Egbue, O.; Long, S. Critical issues in the supply chain of lithium for electric vehicle batteries. *EMJ-Eng. Manag. J.* **2012**, *24*, 52–62. [CrossRef]
40. Banza Lubaba Nkulu, C.; Casas, L.; Haufroid, V.; De Putter, T.; Saenen, N.D.; Kayembe-Kitenge, T.; Musa Obadia, P.; Kyanika Wa Mukoma, D.; Lunda Ilunga, J.M.; Nawrot, T.S.; et al. Sustainability of artisanal mining of cobalt in DR Congo. *Nat. Sustain.* **2018**, *1*, 495–504. [CrossRef]
41. Turcheniuk, K.; Bondarev, D.; Singhal, V.; Yushin, G. Ten years left to redesign lithium-ion batteries. *Nature* **2018**, *559*, 467–470.
42. Li, L.; Zheng, P.; Yang, T.; Sturges, R.; Ellis, M.W.; Li, Z. Disassembly Automation for Recycling End-of-Life Lithium-Ion Pouch Cells. *JOM* **2019**, *71*, 4457–4464. [CrossRef]
43. Cell, Module, and Pack for EV Applications | Automotive Energy Supply Corporation. Available online: http://archive.is/h0BZL (accessed on 2 February 2020).
44. Schmitt, J.; Haupt, H.; Kurrat, M.; Raatz, A. Disassembly automation for lithium-ion battery systems using a flexible gripper. In Proceedings of the IEEE 15th International Conference on Advanced Robotics: New Boundaries for Robotics, ICAR 2011, Tallin, Estonia, 20–23 June 2011; pp. 291–297.

45. Herrmann, C.; Raatz, A.; Mennenga, M.; Schmitt, J.; Andrew, S. Assessment of automation potentials for the disassembly of automotive lithium ion battery systems. In Proceedings of the Leveraging Technology for a Sustainable World—Proceedings of the 19th CIRP Conference on Life Cycle Engineering, Berkeley, CA, USA, 23–25 May 2012; Springer: Berlin/Heidelberg, Germany; pp. 149–154.
46. Hanisch, C.; Loellhoeffel, T.; Diekmann, J.; Markley, K.J.; Haselrieder, W.; Kwade, A. Recycling of lithium-ion batteries: A novel method to separate coating and foil of electrodes. *J. Clean. Prod.* **2015**, *108*, 301–311. [CrossRef]
47. Zhang, G.; He, Y.; Feng, Y.; Wang, H.; Zhang, T.; Xie, W.; Zhu, X. Enhancement in liberation of electrode materials derived from spent lithium-ion battery by pyrolysis. *J. Clean. Prod.* **2018**, *199*, 62–68. [CrossRef]
48. Xin, Y.; Guo, X.; Chen, S.; Wang, J.; Wu, F.; Xin, B. Bioleaching of valuable metals Li, Co, Ni and Mn from spent electric vehicle Li-ion batteries for the purpose of recovery. *J. Clean. Prod.* **2016**, *116*, 249–258. [CrossRef]
49. Li, J.; Shi, P.; Wang, Z.; Chen, Y.; Chang, C.C. A combined recovery process of metals in spent lithium-ion batteries. *Chemosphere* **2009**, *77*, 1132–1136. [CrossRef]
50. Regulation (EC) No 1907/2006 of the European Parliament and of the Council of 18 December 2006 concerning the Registration, Evaluation, Authorisation and Restriction of Chemicals (REACH), establishing a European Chemicals Agency, amending Directive 1999/45/EC and repealing Council Regulation (EEC) No 793/93 and Commission Regulation (EC) No 1488/94 as well as Council Directive 76/769/EEC and Commission Directives 91/155/EEC, 93/67/EEC, 93/105/EC and 2000/21/EC. Available online: https://www.desitek.dk/sites/default/files/media/files/DEHN-REACH-Certificate.pdf (accessed on 8 June 2020).
51. Tait, W.S. Controlling corrosion of chemical processing equipment. In *Handbook of Environmental Degradation Of Materials: Third Edition*; Elsevier Inc., William Andrew Publishing: Norwich, NY, USA, 2018; pp. 583–600. ISBN 9780323524735.
52. Feng, Y.; Siow, K.S.; Teo, W.K.; Tan, K.L.; Hsieh, A.K. Corrosion Mechanisms and Products of Copper in Aqueous Solutions at Various pH Values. *Corrosion* **1997**, *53*, 389–398. [CrossRef]
53. Satyabama, P.; Rajendran, S.; Nguyen, T.A. Corrosion inhibition of aluminum by oxalate self-assembling monolayer. *Anti-Corrosion Methods Mater.* **2019**, *66*, 768–773. [CrossRef]
54. Pernel, C.; Farkas, J.; Louis, D. Copper in organic acid based cleaning solutions. *J. Vac. Sci. Technol. B Microelectron. Nanom. Struct.* **2006**, *24*, 2467–2471. [CrossRef]
55. Nguyen, T. Degradation of Polyfvinyl Fluoride) and Poiyfvinylidene Fluoride). *J. Macromol. Sci. Part C* **1985**, *25*, 227–275. [CrossRef]
56. Diaz, F.; Wang, Y.; Moorthy, T.; Friedrich, B. Degradation Mechanism of Nickel-Cobalt-Aluminum (NCA) Cathode Material from Spent Lithium-Ion Batteries in Microwave-Assisted Pyrolysis. *Metals (Basel)* **2018**, *8*, 565. [CrossRef]
57. Datasheet Gen2 Cell Module, Second life EV Batteries. Available online: https://www.secondlife-evbatteries.com/nissan-leaf-1670wh-module.html (accessed on 7 February 2020).
58. Sahoo, R.N.; Naik, P.K.; Das, S.C. Leaching of manganese from low-grade manganese ore using oxalic acid as reductant in sulphuric acid solution. *Hydrometallurgy* **2001**, *62*, 157–163. [CrossRef]
59. Gorman, S.F.; Pathan, T.S.; Kendrick, E. The 'use-by date' for lithium-ion battery components. *Philos. Trans. R. Soc. A Math. Phys. Eng. Sci.* **2019**, *377*, 20180299. [CrossRef]
60. Lux, S.F.; Lucas, I.T.; Pollak, E.; Passerini, S.; Winter, M.; Kostecki, R. The mechanism of HF formation in $LiPF_6$ based organic carbonate electrolytes. *Electrochem. commun.* **2012**, *14*, 47–50. [CrossRef]
61. Rombach, G. Raw material supply by aluminium recycling-Efficiency evaluation and long-term availability. *Acta Mater.* **2013**, *61*, 1012–1020. [CrossRef]